GEOMETRIC ERROR ASSESSMENT ON SATELLITE IMAGERY FOR GIS ANALYSIS

Kyaw Sann OO*, Masataka TAKAGI**
Department of Infrastructure Systems Engineering
Kochi University of Technology
Tosayamada, Kochi, Japan
*E-mail: 108007u@gs.kochi-tech.ac.jp
**E-mail: takagi.masataka@kochi-tech.ac.jp

***ABSTRACT*:** Imagination of earth-surface's objects is contaminated with errors by sensor to target acquisition systems in the satellite remote sensing. Movement of the sensor and displacement of the target are propagated geometric error on the imagery. Systematic errors could be removed by trajectory model and rigorous sensor model; however, random errors are existed that in which is difficult to remove without affecting to image geometry. The study introduced geometric error assessment (GEA) on image objects to understand the error geometries from the imagery. At first, ground control points (GCP) and check points (CP) are scattered in all direction of the image. Then, errors are generated seeding the GCP location using Box-Muller method. The method produced simulated GCP contaminated with errors. Random errors are subtraction from simulated GCP by the true one. The study found that the error of CP is approached to zero when the CP closed to GCP. The corrected image would be applied for GIS analysis such as land-use/land-cover mapping and management, disaster risk mapping and management, urbanization prediction and management, water resource management.

KEYWORDS: Geometric error, GCP, check points, random error

1. INTRODUCTION

Surveyors and engineers are believes that errors are propagated in all kind of measurements (Charles D. Ghilani, 2006). The errors could be systematic errors or random errors. Systematic errors could be removed by applying related physical conditions and correct measurement procedures; however, random errors are complex and it is the arduous work to remove the random errors. Despite the fact the random errors could be the least by understanding the geometry of errors and iterating the observations (Charles D. Ghilani, 2006). The geometry of random errors was generated from the simulated ground control points (GCP) and check points (CP). Iterated error generation processes were applied when simulating GCP and CP. Random values are generated by Box-Muller method and it provides the random values from the standardized Gaussian distribution *N(0,1)* (Cox et al., 2001). The generated random values are added to the true value of control points. By iterating the transformation process with generated random errors, the geometry of errors was calculated. The study compares that error geometry between 3D affine transformation and 3D projective transformation. The different distributions of GCP and CP also demonstrated. The approach of this study investigated that the geometry and distribution of random errors in ALOS PRISM image to the least

of the random errors propagation. The result image could be used in the processes of location based monitoring and analysis such as land-use/land-cover mapping and management, disaster risk mapping and management, urbanization prediction and management, water resource management.

2. Methodology

There are three datasets used to implement this study. They are IKONOS image as reference data, elevation data from DSM (RaMSE: Kokusai kogyo CO., LTD.) data and the target image of ALOS PRISM. In the study, we assumed that the location of IKONOS image is true and DSM's high value also acquired based on it.

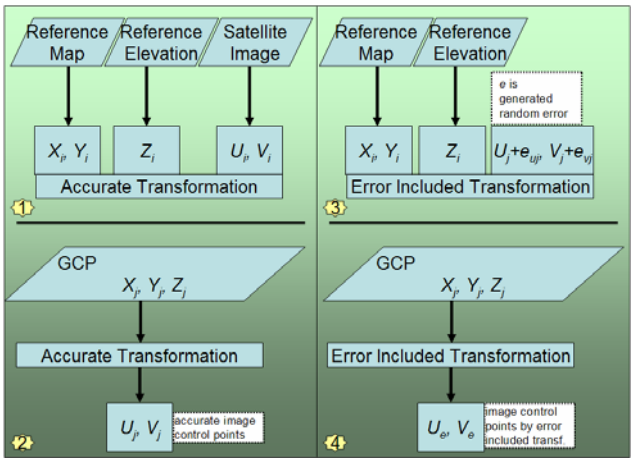

Figure 1: The general flow of methodology

There four mains steps in the procedure (figure 1). *X* and *Y* values are collected from reference IKONOS image and *Z* values are from the DSM data. Assume U_i and V_i data are collected from target ALOS's PRISM data visually. True values U_j and V_j are produced by transform function (equation 1). In other side, generated errors (e_{uj},e_{vj}) are added to the assume image control points. The process of errors contamination was iterated to 20 times.

$$U_t = f_u(x, y, z)$$
$$V_t = f_v(x, y, z) \quad (1)$$

where U_t, V_t are true values; $f_u(x, y, z)$ and $f_v(x, y, z)$ are transform function for assume *u* and *v*.

2.1 GCPs and Check Points

From sample datasets, ground control points (GCP) and check points (CP) are visually interpreted as assume control points. They are well distributed (figure 2) in the sample area. Each control points could be recognized in both of target and reference image.

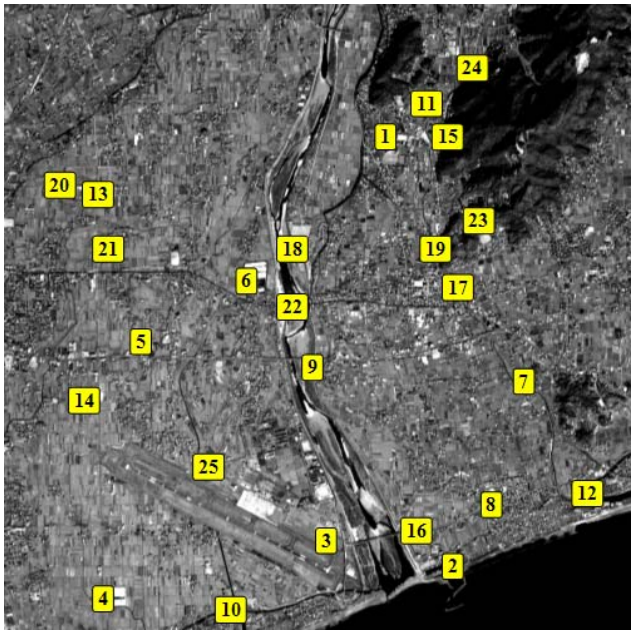

Figure 2: Location distribution of control points

By inserting coordinates of GCP and PC to the equation 1, a pair new transformation function (equation 2 &3) is produce.

For GCP, transformed function can be

$$U_{gcp} = f_u(x, y, z)$$
$$V_{gcp} = f_v(x, y, z). \quad (2)$$

For CP, transform function can be

$$U_{cp} = f_u(x, y, z)$$
$$V_{cp} = f_v(x, y, z). \quad (3)$$

The transform function will be changed base on the method of transformation. Two transformation methods are applied in this study. Prior to the transformation, random errors intruded true control points (GCP and CP) are generated by adding the true values and generated random values.

2.2 Method of random error generation

Box-Muller transformation (equation 4) generated a pair of independent standard uniformly distributed random numbers from the standardized Gaussian distribution *N(0,1)*. Suppose U_1 and U_2 are independent random variables that are uniformly distributed in the interval *(0,1)*; then, X_0 and X_1 are independent random variables with a normal distribution of standard deviation 1.

$$X_0 = \sqrt{-2lnU_1}\cos(2\pi U_2)$$
$$X_1 = \sqrt{-2lnU_1}\sin(2\pi U_2) \qquad (4)$$

Random errors were generated using this algorithm. Let u_g and v_g are independent random errors with mean of true GCPs of standard deviation 1. The Box-Muller random variable generator is generated random error with specific mean *u* and *v* (equation 5).

$$u_g = \sqrt{-2lnU_1}\cos(2\pi U_2) + u$$
$$v_g = \sqrt{-2lnU_1}\sin(2\pi U_2) + v \qquad (5)$$

where u_g and v_g are x, y coordinate of simulated random error intruded control points; and *u* and *v* are true location of the coordinate control points. This generation process was iterated for 20 times, producing 20 pairs of simulated control points.

If we substitute coordinate of control points to the equation 5, the random error contaminated control points are calculated (equation 6&7).

For GCP,

$$u'_{gcp} = \sqrt{-2lnU_1}\cos(2\pi U_2) + U_{GCP}$$
$$v'_{gcp} = \sqrt{-2lnU_1}\sin(2\pi U_2) + V_{GCP} \qquad (6)$$

and for CP,

$$u'_{cp} = \sqrt{-2lnU_1}\cos(2\pi U_2) + U_{CP}$$
$$v'_{cp} = \sqrt{-2lnU_1}\sin(2\pi U_2) + V_{CP} \qquad (7)$$

The simulated control points are generated using the equations 7&8. 20 pairs of control points are simulated by iterating 20 times. This iteration data will be the basic requirement for random error geometry investigation.

2.3 Method of transformation

Amount several types of transformation methods, the study selected 3D affine and 3D projective transformation methods based on effectiveness of them.

In general, 3D affine transformation function can be represented by the equation 8.

$$u = ax + by + cz + d$$
$$v = ex + fy + gz + h \qquad (8)$$

And, 3D Projective transformation function can be represented by equation 9.

$$u = (a_1x+a_2y+a_3z+a_4)/(b_1x+b_2y+b_3z+1)$$
$$v = (a_5x+a_6y+a_7z+a_8)/(b_1x+b_2y+b_3z+1) \qquad (9)$$

Based on parameter requirements of these functions, we selected 25 control points including 11 GCP and 14 CP scattering in the image. There four types of pattern distribution (figure 3) are using in transformation process to investigate the influent of

ground condition to error geometry.

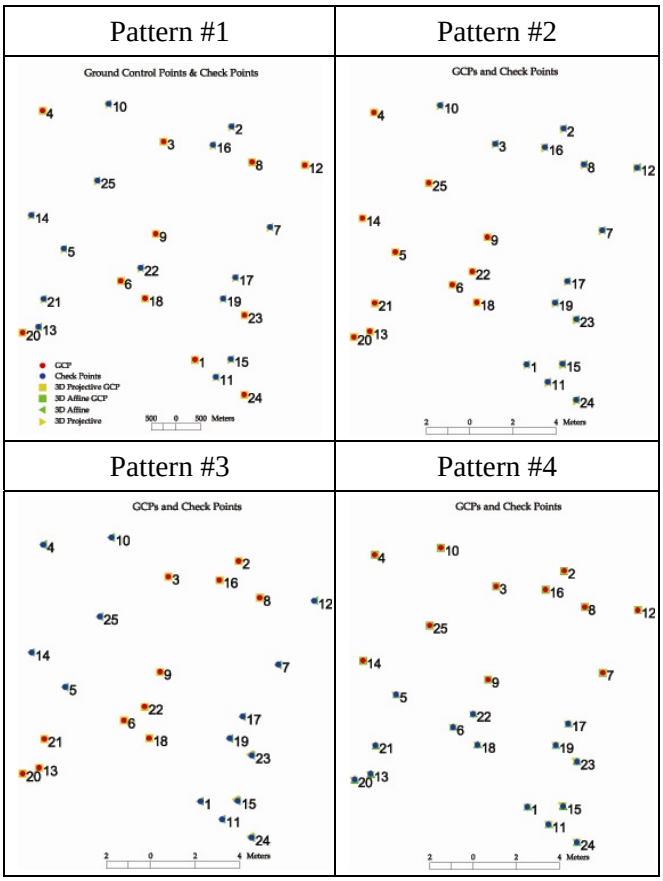

Figure 3: Distributions of GCP and CP

In distributions, pattern 1 is well distributed over the image; while others had less scattering. Pattern 2's image control points are selected in the non-elevated plain and it is located in the right side of image. When pattern 4 is distributed in the elevated area pattern 3 is distributed diagonally ranging from elevated area through plain with narrow distribution.

In other hand, the propagated errors could be calculated.

2.4 Error propagation

The computational process into the new values can be propagated with the errors that were presented in the original direct observations. Therefore, the functions of the original errors could be containing as indirectly in next measurements (Charles D. Ghilani, 2006). By definition, the difference of a true value and its measured value is an error. Suppose, ε is the error in an observation, y is the measured value, and μ its true value, then

$$\varepsilon = y - \mu. \qquad (10)$$

The equation 10 will yield a new equation, if you substitute coordinate of control points.

$$\varepsilon_u = U_t \pm U'$$
$$\varepsilon_v = V_t \pm V' \qquad (11)$$

where U_t, V_t is true value and U', V' is simulated control points.

3. RESULT

There are 20 times of 25 control points (11 GCP and 14 check points) were generated with different distribution patterns. By locating all those error coordinates, the vectors of error geometry are calculated. The vectors are originated in true coordinate; then headed the direction trend of errors. After magnified the vectors by 100 times the geometries of vector are distinct to the view (figure 5). In all four patterns, red dots represent GCP; blue dots represent control points; green arrows represent 3D affine error vectors; and golden errors represent 3D projective error vecotors. In other hand, there are four distribution patterns are used to input to the two kinds of selected transformation functions (3D affine and 3D projective transformation).

In the results of root mean squares error (RMSE), the well distributed ground control points (GCP) produced the least RMSE comparing with others distribution patterns. The orientation of high changed the vector of errors. The result shows that aggregated ground control points (GCP) contributed

low potential to far check points. Uneven ground condition reflected more complex error geometry.

Error Vector on Pattern #1

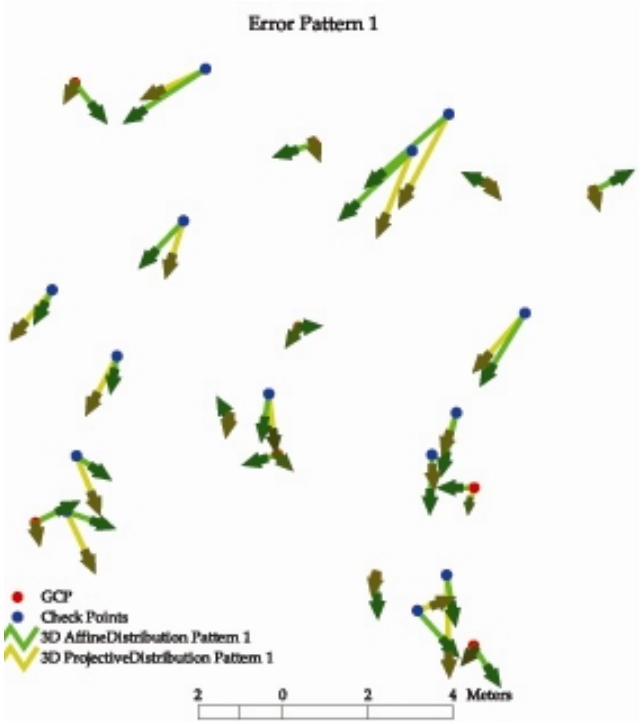

Error Vector on Pattern #2

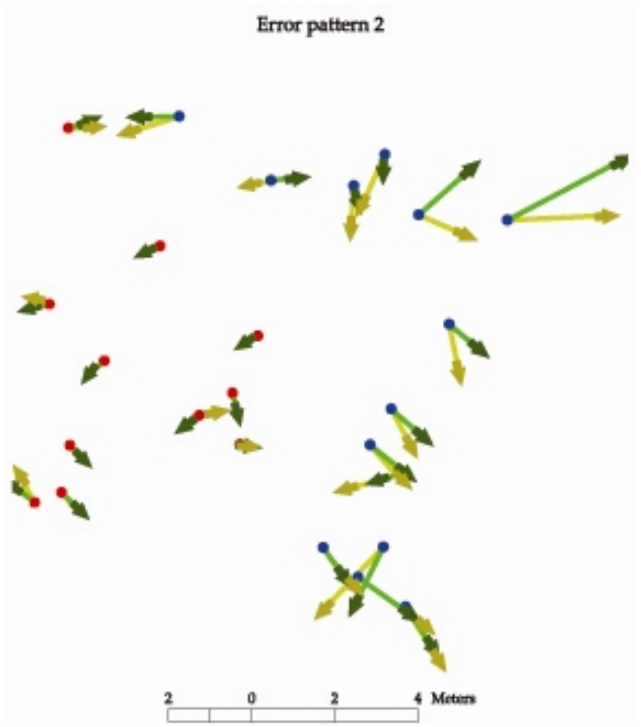

Error Vector on Pattern #3

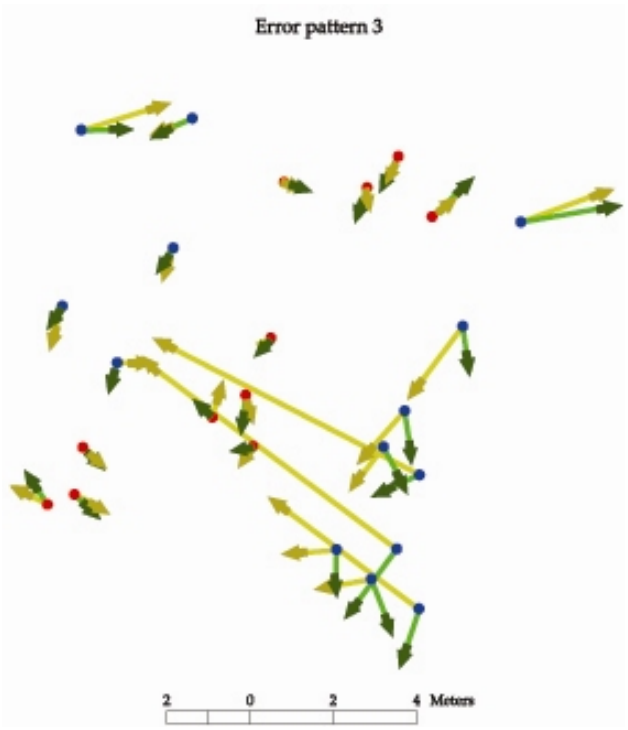

Error Vector on Pattern #4

Figure 5: Error vectors of each distribution

As of transformations processes, 3D projective transformation gives more precision than 3D affine in whatever GCP or CP. Apart from control points and transformation methods, the study proved that the selection and distribution pattern have positively related with condition for ground elevation.

4. DISCUSSION

Pattern 1, well distributed control points, had more precision consistency than others for both of transformation. Pattern 2, GCPs from non-elevated area, precision consistency is high around GCPs when CPs had low precision. Pattern 3, narrow distribution GCPs, high accuracy around GCPs. Unexpectedly, 3D affine transformation had more potential around CPs. Pattern 4, GCPs from elevated area, there are low precision for some GCPs.

The reference IKONOS image may be intruded original errors. The removal of it will be another task.

5. FUTURE WORK

By using VRS-GPS GCPs, the errors of reference data were minimized to the VRS-GPS standard. The next step of the study will be worked along the ALOS's PRISM and AVNIR II datasets to get VRS-GPS standard precision. Then, more transformation methods will be applied to find the potential of transformation models.

REFERENCES

Cox, M. G., Dainton, M.P., Harris, P.M. 2001. *Software Specifications for Unvertainty Calculation and Associated Statistical Analysis*, NPL Report CMSC 10/01.

Ghilani, Charles D., and Paul R. Wolf. 2006. *Addustment Computation: spatial data analysis*, 4th ed., John Wiley & Sons, Inc., Hoboken, NJ.

Hastedt, H., 2006. (2006). *Monte-Carlo-Simulation in close-range photogrammetry*, The International Archives of the Photogrammetry, Remote Sensing and Spatial Information Sciences, Vol. 34, Part XXX[CD-ROM].

Richards, J. A., *Remote Sensing Digital Image Analysis*, Springer-Verlag, Berlin, 1999.

Russ, John C., *The image processing handbook*, CRC Press, Inc., USA, 1995.

Takeshi MIYATA, Jong Hyeok JEONG and Masataka TAKAGI, (2006).*Extracting Method of Mudflow Disaster by using Arial Photography*, Proceedings of International Symposium on Management Systems for Disaster Prevention, JAPAN.

Masataka TAKAGI, Lecture on Survey 1, section 7, "*Vector*".

Masataka TAKAGI, Lecture on Survey 2, section 10, "*Transformation*"